

Data Supplement to:

Genome-Wide Transcriptional Profiling Reveals Connective Tissue Mast Cell Accumulation in Bronchopulmonary Dysplasia.

¹Soumyaroop Bhattacharya, ¹Diana Go, ¹Daria L Krenitsky, ¹Heidi L Huyck, ¹Siva Kumar Solleti, ¹Valerie A Lunger, ²Leon Metlay, ³Sorachai Srisuma, ⁴Susan E Wert, ¹Thomas J Mariani* and ¹Gloria S Pryhuber*

Departments of ¹Pediatrics and ²Pathology, University of Rochester Medical Center, 601 Elmwood Ave, Box 850, Rochester, NY 14642, USA, ³Department of Physiology, Faculty of Medicine Siriraj Hospital, Mahidol University, Bangkok, Thailand and Perinatal Institute, ⁴Cincinnati Children's Hospital Medical Center, Cincinnati, OH 45229.

*Corresponding Authors

7 Figures

2 Tables

3 Supplemental Figures

4 Supplemental Tables

Address for Correspondence:

Gloria S Pryhuber, MD
Division of Neonatology,
Department of Pediatrics,
University of Rochester Medical Center,
601 Elmwood Ave, Box 850,
Rochester, NY 14642,
USA

Thomas J Mariani, PhD
Division of Neonatology and
Center for Pediatric Biomedical Research
University of Rochester Medical Center,
601 Elmwood Ave, Box 850,
Rochester, NY 14642,
USA

Running Title: Genome-Wide Expression in BPD

Keywords: microarray, tryptase, chymase, carboxypeptidase A3, BPD

Funding support: University of Rochester Clinical and Translational Science Institute (NIH UL1 RR024160-03), University of Rochester Strong Children's Research Center, NIH T32HD057821

Supplemental Table 1: Primer sequences and assay information for qPCR validation performed in this study. Shown are gene ID, forward and reverse primer sequences, or assay ID for commercial assays.

Gene	Forward Primer	Reverse Primer
<i>SYBR Assay</i>		
<i>Human</i>		
PPIA	CCCACCGTGTCTTCGACATT	GGACCCGTATGCTTAGGATGA
IGF1	ATGCTCTCAGTTCTGTGTG	GGGCTGATACTCTGGTCTT
CCL17	CTTCTCTGCAGCACATCCAC	CTGCCCTGCACAGTTACAAA
CEACAM5	CCCAGACTCGTCTAACCTGC	TTGGCGATAAAGAGAACTTGTGT
CEACAM6	TCCCCCTCAAAGGCCAATTAC	TGGAACGTCCCATTGATAAAC
SLC27A6	ACTCCGTATGCCATTCCAA	TTGGAGAACTTGTCGCTACC
FABP4	AGCACCATAACCTTAGATGGGG	CGTGGAAAGTGACGCCCTTCA
SFN	AGGCCGAACGCTATGAGGA	GGTTTCGCTTCGCAGGA
COL8A1	GCTGCCACCTCAAATTCTC	CAGGGGCTGGTATTGTGGA
HHIP	CTTTGGCCCTGACGGCTT	GTAGCACTGAGCCTGTGAAATC
TEK	TGCCACCCCTGGTTTACGG	TTGGAAGCGATCACACATCTC
CPA3	GGGTTTGATTGCTACCACTCTT	GCCAAGTCCTTATGATGTC
TPSB2	CCCGCACCGATACTGGATG	GATCTGGCGGTGTAGAACT
TPSAB1	GTGACGCAAAATACCACCTTGGC	CCATTACCTTGACACCAGGG
KITLG	AATCCTCTCGTAAAAGTGAAGG	CCATCTGCTTATCCAACAATGA
IL4	CGGCAACTTGTCCACCGA	TCTGTTACGGTCAACTCGGTG
GRP	AAAGAGCACAGGGAGTCTC	TCCTTGCTTCTATGAGACCCA
<i>Mouse</i>		
CPA3	AATTGCTCCTGTCCACTTGAC	TCACTAACTCGGAAATCCACAGT
TPSB2	CTGGCTAGTCTGGTGTACTCG	ATGCCCACTCGCTGATTGG
TPSAB1	GCCAATGACACCTACTGGATG	GAGCTGTACTCTGACCTTGTG
<i>Taqman Assay</i>		
<i>ABI Assay ID</i>		
PPIA	Hs04194521_s1	
CXCL5	Hs00171085_m1	

Supplemental Table 2: Gene expression data for a subset of "vascular-related" genes in BPD tissue as compared to controls. Shown are gene symbol, probe set ID, fold-change (BPD/control) and p-value as defined by student's t-test, for representative measures. Although magnitude changes are small, likely diluted by non-vascular cells, we observed a general decrease in expression of vascular markers.

<i>Genes</i>	<i>Probe sets</i>	<i>P Value</i>	<i>Fold Change</i>
HIF3A	222123_s_at	0.05	0.50
FLT1	204406_at	0.09	0.77
NOS1	1560974_s_at	0.21	0.79
NOS2	210037_s_at	0.02	0.82
TIE2	206702_at	0.02	0.82
NOS3	205581_s_at	0.41	0.88
PECAM1	208983_s_at	0.31	0.91
ENG	201808_s_at	0.68	0.94
VEGF	212171_x_at	0.67	0.94
ANG1	205608_s_at	0.59	1.08
HIF1A	200989_at	0.06	1.13

Supplemental Table 3: Genes significantly affected in BPD lung tissue. Shown are gene symbol, probe set ID, fold-change (BPD/control) and p-value as defined by student's t-test, for 159 genes.

Genes	Probe set	P Value	Fold Change
CPA3	205624_at	2.27E-03	7.25
CCL18	32128_at	1.95E-03	6.73
IGHA1	217022_s_at	1.94E-02	6.69
TPSB2	207134_x_at	5.65E-03	5.25
TPSAB1	205683_x_at	4.88E-03	5.15
ALDH1A3	203180_at	2.25E-03	4.54
IGHM	211430_s_at	8.02E-02	4.37
PLUNC	220542_s_at	3.47E-02	4.17
FABP4	203980_at	8.77E-03	4.16
DNAJC5B	232798_at	8.24E-03	4.03
ATP6V0D2	1553155_x_at	8.54E-03	3.72
CXCL13	205242_at	3.60E-02	3.64
EREG	205767_at	9.83E-03	3.28
CEACAM5	201884_at	1.66E-02	3.17
COMP	205713_s_at	9.43E-03	3.02
C20ORF114	226067_at	9.41E-02	2.98
IGJ	212592_at	1.81E-02	2.95
CH25H	206932_at	1.84E-02	2.84
LGALS3	1557197_a_at	9.13E-03	2.83
SFN	33323_r_at	2.96E-02	2.79
IGL@	215214_at	6.29E-02	2.78
COL8A1	214587_at	1.97E-04	2.72
RBP4	222049_s_at	5.51E-02	2.72
TDO2	231702_at	2.15E-02	2.67
HDC	207067_s_at	8.44E-03	2.58
MSMB	207430_s_at	1.39E-01	2.56
INHBA	210511_s_at	2.22E-02	2.55
ASPM	219918_s_at	4.88E-03	2.50
STEAP1	205542_at	9.45E-03	2.49
NNMT	202238_s_at	4.02E-03	2.47
PCOLCE2	219295_s_at	8.37E-02	2.46
IGKC	215217_at	1.75E-01	2.45
PBK	219148_at	2.11E-02	2.44
PAPPA	224942_at	4.72E-02	2.42
CEACAM6	211657_at	5.82E-04	2.40
CD8A	205758_at	1.16E-01	2.39
NEIL3	219502_at	3.92E-03	2.38
APOC2	231562_at	3.09E-02	2.35
SIGLEC6	206519_x_at	1.99E-02	2.34
RRM2	209773_s_at	5.62E-03	2.34

APOBEC3B	206632_s_at	1.06E-02	2.32
C6ORF105	229070_at	3.13E-02	2.32
PSCA	1560011_at	1.10E-03	2.31
ADAMTS16	238125_at	2.20E-02	2.30
GREM1	218469_at	8.91E-02	2.29
IL1RL1	242809_at	2.05E-01	2.29
DOK5	214844_s_at	2.82E-03	2.29
CXCL5	215101_s_at	6.16E-02	2.29
DKK1	204602_at	4.06E-02	2.28
CDK1	231534_at	2.91E-03	2.28
CGA	204637_at	6.86E-02	2.28
DEPDC1	222958_s_at	9.66E-03	2.26
SELE	206211_at	1.58E-01	2.26
GPR109B	205220_at	3.74E-02	2.25
CHIT1	208168_s_at	5.80E-03	2.23
P4HA3	228703_at	1.33E-02	2.22
DIO2	203700_s_at	2.69E-03	2.21
IGK@	221651_x_at	1.47E-01	2.21
SERPINA1	230318_at	5.78E-02	2.20
ACP5	204638_at	7.05E-02	2.20
PLA2G2A	203649_s_at	1.07E-01	2.20
BHLHE22	228636_at	1.61E-01	2.20
TTK	204822_at	8.40E-03	2.19
C7ORF68	1554452_a_at	2.15E-02	2.19
SLC18A2	205857_at	1.38E-02	2.18
TMTC1	224397_s_at	2.21E-02	2.18
KIF14	236641_at	3.11E-03	2.18
KIF18B	222039_at	1.93E-02	2.18
CA12	203963_at	1.66E-02	2.18
SFRP2	223122_s_at	1.42E-01	2.17
KRT17	205157_s_at	1.49E-01	2.16
ADORA3	223660_at	7.77E-02	2.15
TARP	211144_x_at	5.10E-02	2.15
SKA1	217640_x_at	8.40E-03	2.15
CD5L	206680_at	3.23E-02	2.14
MXRA5	209596_at	8.70E-02	2.14
DLGAP5	203764_at	1.16E-02	2.14
CDCP1	218451_at	2.31E-02	2.14
BUB1	209642_at	2.74E-03	2.14
ANLN	1552619_a_at	1.05E-02	2.14
C1QB	202953_at	3.46E-02	2.14
KIAA0101	202503_s_at	7.27E-03	2.13
KMO	205306_x_at	3.22E-02	2.13
LIPG	219181_at	1.48E-01	2.12
CDC25C	205167_s_at	1.18E-02	2.12
MS4A2	207496_at	3.05E-02	2.12

TNIP3	220655_at	1.38E-02	2.11
C1QA	218232_at	2.81E-02	2.10
IL17RB	224156_x_at	1.20E-02	2.10
THEMIS	1558972_s_at	1.29E-01	2.10
CD177	219669_at	1.94E-01	2.10
CENPA	204962_s_at	1.40E-02	2.09
MKI67	212023_s_at	1.23E-02	2.09
KIF23	244427_at	2.23E-03	2.09
HS3ST2	219697_at	2.48E-02	2.09
MND1	223700_at	5.08E-03	2.08
C10ORF10	209182_s_at	5.14E-02	2.08
POSTN	1555778_a_at	3.37E-02	2.08
HLA-DRB4	209728_at	4.81E-01	2.08
ADCYAP1	230237_at	1.18E-01	2.08
CCDC102B	220301_at	1.22E-02	2.06
ARNTL2	220658_s_at	2.86E-02	2.06
SIGLEC1	219519_s_at	4.98E-02	2.05
BIRC5	202094_at	1.76E-02	2.05
IQGAP3	229538_s_at	4.34E-02	2.05
TPX2	210052_s_at	6.15E-03	2.05
IGF1	209542_x_at	8.90E-03	2.03
SPC25	209891_at	3.00E-02	2.03
CDKN3	209714_s_at	6.98E-03	2.02
DHRS9	219799_s_at	1.91E-02	2.02
CYP24A1	206504_at	3.11E-02	2.02
TOP2A	201291_s_at	1.82E-02	2.02
LIF	205266_at	1.16E-01	2.02
SH3RF2	228892_at	7.57E-03	2.02
TMEM158	213338_at	2.15E-02	2.02
DIAPH3	220997_s_at	7.49E-03	2.01
NEK2	204641_at	8.27E-03	2.01
MARCO	205819_at	1.17E-01	2.00
POU2AF1	1569675_at	9.41E-02	0.50
ADCYAP1R1	226690_at	6.13E-02	0.50
CA4	206209_s_at	6.51E-04	0.50
LRRC15	213909_at	1.37E-01	0.49
RORC	228806_at	6.18E-03	0.49
AGER	210081_at	1.28E-02	0.48
COL4A6	213992_at	7.68E-03	0.48
UGT2B17	207245_at	9.48E-02	0.48
RTKN2	230469_at	9.16E-02	0.47
XIST	221728_x_at	5.58E-01	0.47
SOX11	204913_s_at	5.48E-02	0.47
KCNJ16	219564_at	4.91E-02	0.47
HHIP	1556037_s_at	3.44E-02	0.47
ALPP	204664_at	1.03E-02	0.47

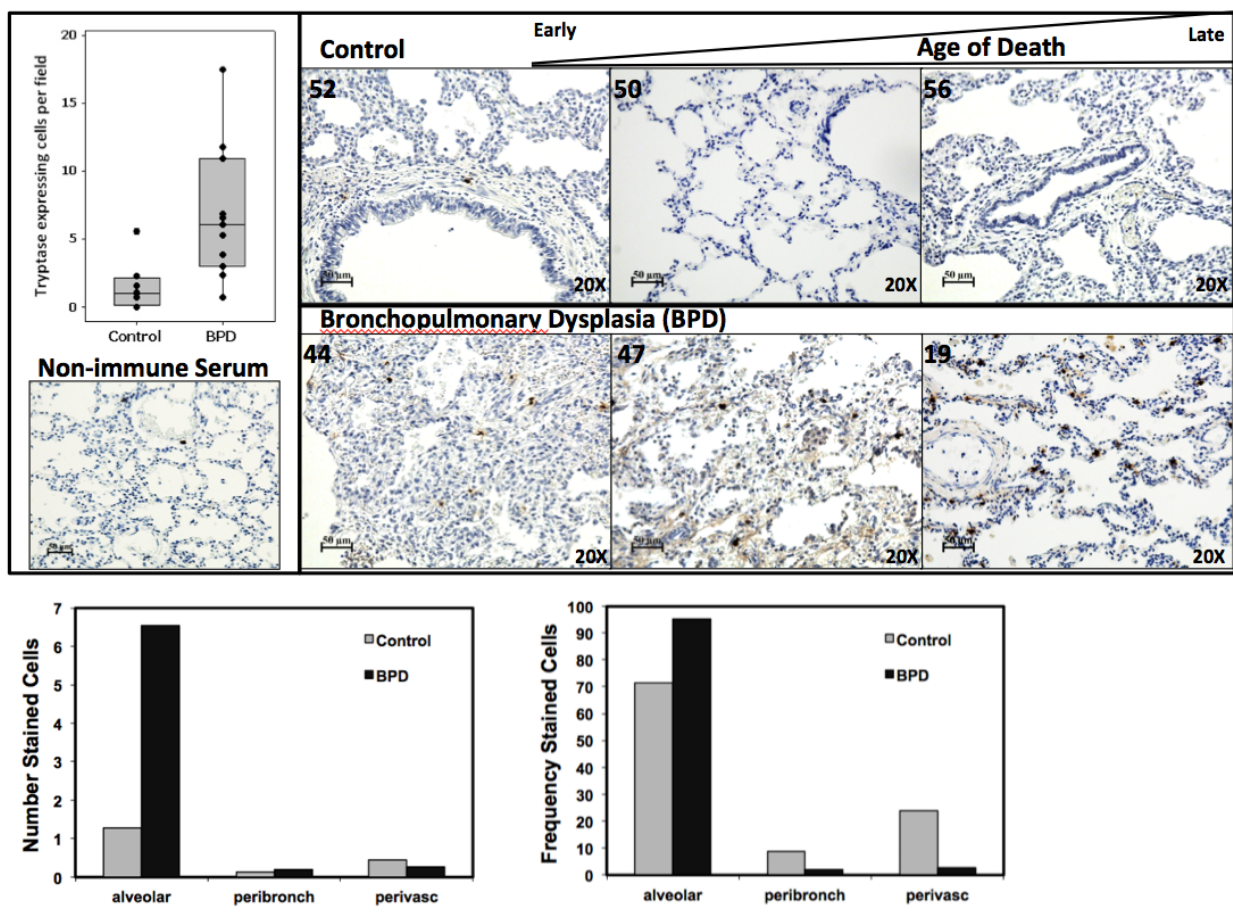
FABP6	210445_at	9.35E-03	0.47
KANK4	229125_at	3.42E-04	0.46
SLC27A6	219932_at	1.02E-03	0.46
PRND	222106_at	2.65E-01	0.45
FCER1A	211734_s_at	1.78E-02	0.43
TTLL6	230924_at	3.36E-04	0.43
GHRL	223862_at	1.26E-01	0.42
CSMD1	231223_at	1.22E-02	0.41
CCL22	207861_at	2.28E-02	0.41
AADAC	205969_at	4.54E-02	0.41
CCL17	207900_at	4.50E-04	0.41
APOH	205216_s_at	2.54E-02	0.40
GPIHBP1	238062_at	7.14E-02	0.39
LRRC2	219949_at	2.16E-02	0.39
GSTT1	232193_at	1.06E-02	0.39
LPPR1	219732_at	3.34E-02	0.39
SLC44A5	235763_at	9.88E-03	0.39
SOSTDC1	213456_at	1.39E-02	0.38
S100A3	206027_at	6.59E-03	0.37
UPK3B	206658_at	9.10E-03	0.36
SLCO1A2	211480_s_at	3.67E-02	0.33
OLFM3	1554524_a_at	1.43E-02	0.32
ANXA8L2	203074_at	1.51E-02	0.31
VGLL1	215729_s_at	6.71E-03	0.31
EDN3	208399_s_at	4.52E-02	0.28
ITLN1	223597_at	4.14E-02	0.28
PSPH	205048_s_at	8.37E-02	0.26

Supplemental Table 4: qPCR validation of IL4, GRP and KITLG expression in human lung tissue. Shown are mean fold-change (\pm standard deviation) in each group, non-BPD control (CTL) or BPD, relative to the control population. IL4 expression was not detectable in lung tissue from either group. GRP and KITLG expression were detectable in all lung tissues, but no differences in BPD subjects were observed.

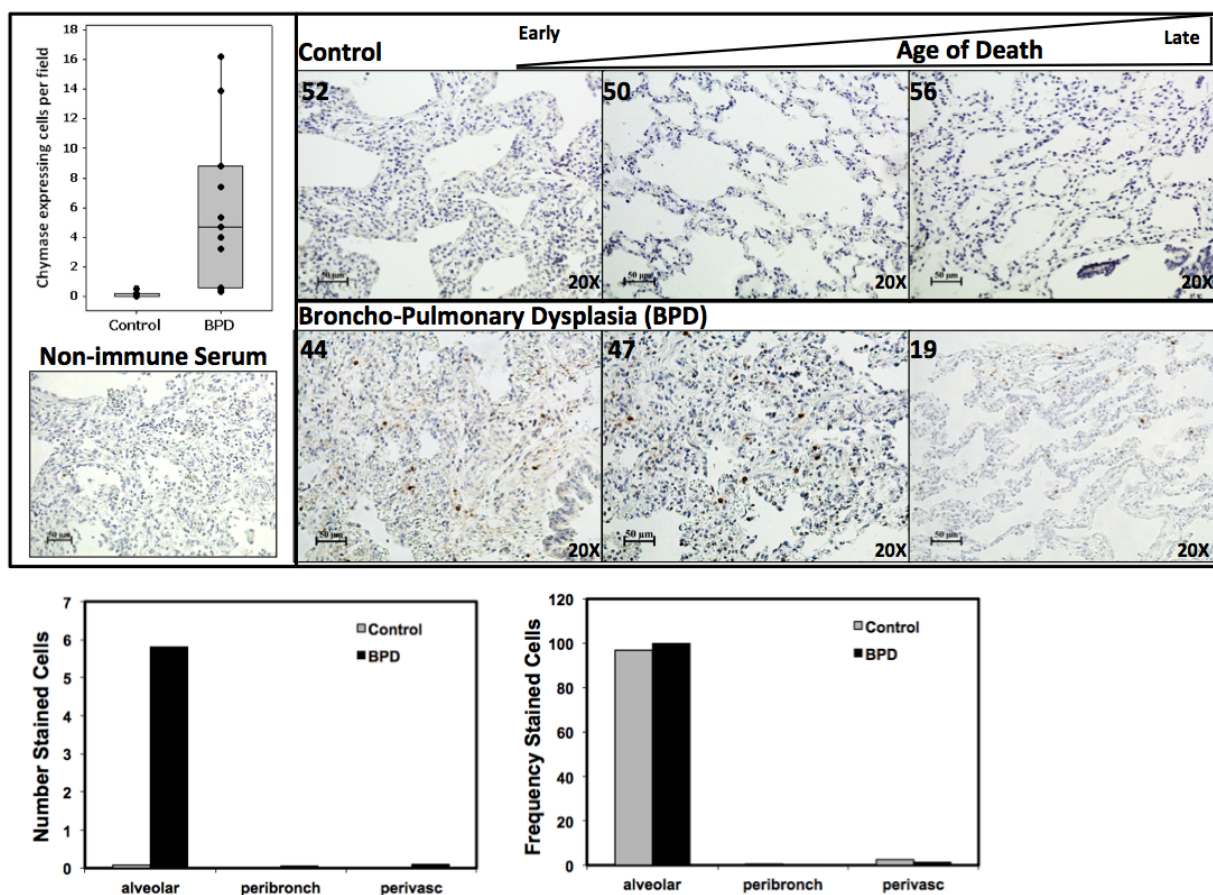
	<i>Control</i>	<i>BPD</i>	
IL4	ND	ND	ND
GRP	1.26 (\pm 0.96)	1.70 (\pm 1.28)	p>>0.05
KITLG	1.21 (\pm 0.67)	1.06 (\pm 0.55)	p>>0.05

ND = Not Detectable

Supplemental Figure 1. We used immunohistochemistry to identify tryptase, a general mast cell-specific marker. Quantitative analysis of the number of tryptase-expressing cells in BPD and non-BPD control lungs is indicated at the top left. Shown are the average numbers of stained cells/field for each individual subject (dots), the group means (bar) and interquartile range (box). Individual images show staining patterns in corrected gestational age matched control and BPD subjects (subject ID indicated). Panels are arranged according to gestational age at death. Also shown is an absence of staining in non-immune serum controls. Bar graphs at bottom show distribution of stained cells within the alveolar, peribronchiolar or perivascular region of BPD and control tissues. Data are presented as the average absolute number of cells per subject in each region (bottom left) or the frequency (proportion) of stained cells found in each region (bottom right).



Supplemental Figure 2. We used immunohistochemistry to identify chymase, a specific marker for connective tissue-type mast cells. Quantitative analysis of the number of chymase-expressing cells in BPD and non-BPD control lungs is indicated at the top left. Shown are the average numbers of stained cells/field for each individual subject (dots), the group means (bar) and interquartile range (box). Individual images show staining patterns in corrected gestational age matched control and BPD subjects (subject ID indicated). Panels are arranged according to gestational age at death. Also shown is an absence of staining in non-immune serum controls. Bar graphs at bottom show distribution of stained cells within the alveolar, peribronchiolar or perivascular region of BPD and control tissues. Data are presented as the average absolute number of cells per subject in each region (bottom left) or the frequency (proportion) of stained cells found in each region (bottom right). Bar graphs at bottom show distribution of stained cells within the alveolar, peribronchiolar or perivascular region of BPD and control tissues. Data are presented as the average absolute number of cells in each region (bottom left) or the frequency of stained cells found in each region (bottom right).



Supplemental Figure 3. We used immunohistochemistry to identify chymase, a specific marker for connective tissue-type mast cells, in a mouse model of BPD-like lung injury. Chymase expressing cells were observed in lung tissue from FGFR3/4 deficient mice at 1 month of age (B, D, F), but rarely in age-matched, littermate control lungs (A, C). No staining was detected in control sections stained with pre-immune serum (E). Original magnification = 200X.

